Designing 3D Object Rendering Techniques for Ultrasound Mid-Air Haptics using Intersection Strategies

Lendy Mulot*
lendy.mulot@irisa.fr
Univ Rennes, INSA, IRISA
Rennes, France

Thomas Howard*
thomas.howard@irisa.fr
Univ Rennes, INSA, IRISA
Rennes, France

Sarah Emery
sarah.emery@ens-rennes.fr
Univ Rennes, ENS Rennes
Rennes, France

Claudio Pacchierotti
claudio.pacchierotti@irisa.fr
CNRS, Univ Rennes, Inria, IRISA
Rennes, France

Maud Marchal
maud.marchal@irisa.fr
Univ Rennes, INSA, IRISA and IUF
Rennes, France

ABSTRACT

Ultrasound mid-air haptic (UMH) interfaces focus acoustic energy to generate high-pressure focal points in mid-air, creating tactile sensations. When these focal points are modulated over time, they can render tactile patterns with various properties in a 3D workspace. While UMH has been used to render curves and 2D shapes, such as tactile icons, rendering 3D objects in full is nowadays an open problem, as it would require more powerful devices. To overcome this limitation, designers typically only render a representation of the intersection between the user's hand and the virtual object. However, there is no consensus in the literature on how best to compute this intersection.

This paper formalizes a pipeline for computing the intersection between a user's hand and a 3D virtual object. Together with state-of-the-art sampling strategies, this forms an end-to-end design process for rendering 3D objects with UMH. A user study demonstrates the significant impact of intersection strategy design choices on the perception of 3D object properties, specifically infill density. We illustrate that different strategies can alter the perception of how hollow or filled an object is, which can be challenging to render in mid-air. By providing a standardized way to report and study 3D object rendering with UMH, this work aims to facilitate and motivate further exploration of perceptual effects via UMH technologies.

CCS CONCEPTS

• **Human-centered computing** → **Haptic devices**; **User studies**.

KEYWORDS

Ultrasound Haptics, Mid-Air Haptics, Haptic Perception

ACM Reference Format:
Lendy Mulot, Thomas Howard, Sarah Emery, Claudio Pacchierotti, and Maud Marchal. 2024. Designing 3D Object Rendering Techniques for Ultrasound Mid-Air Haptics using Intersection Strategies. In *ACM Symposium on Applied Perception 2024 (SAP '24), August 30–31, 2024, Dublin, Ireland*. ACM, New York, NY, USA, 8 pages. https://doi.org/10.1145/3675231.3675235

*Both authors contributed equally to this research.

SAP '24, August 30–31, 2024, Dublin, Ireland

ACM ISBN 979-8-4007-1061-2/24/08
https://doi.org/10.1145/3675231.3675235

1 INTRODUCTION

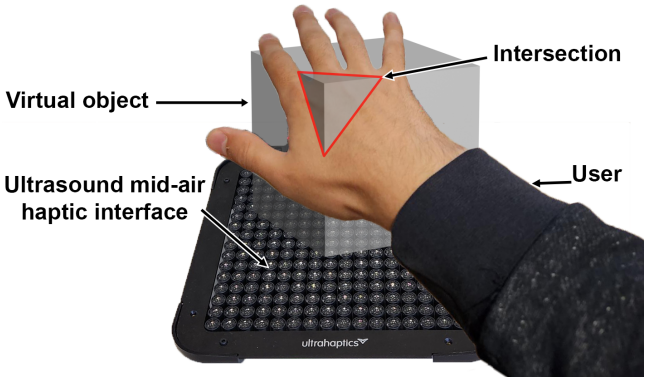

Figure 1: Exploration of a virtual 3D object rendered with an ultrasound mid-air haptic interface. When representing 3D objects with mid-air technologies, we generally render their intersection with the user's hand.

Ultrasound mid-air haptic (UMH) interfaces have gained a great deal of interest due to the large amount of control they provide haptic designers with. They are also very convenient to use as they do not require the user to wear any equipment, leading to natural interactions [Rakkolainen et al. 2021].

UMH interfaces [Carter et al. 2013; Iwamoto et al. 2008] are composed of an array of ultrasound transducers, whose phase can be independently controlled to constructively interfere on a point in mid-air. This locally creates a high-pressure focal point that vibrates at the frequency of the ultrasound wave (usually 40 kHz or 70 kHz). Upon reaching a focal point, the high pressure will slightly indent the skin, creating a vibro-tactile stimulus. The interface can then be controlled to change the position of the focal point [Hoshi et al. 2009].

Given that the very high vibration frequency of the vibration is above the upper limit of the sensitivity range of Pacinian corpuscles, a focal point cannot be perceived as is [Verrillo 1966]. Thus, two approaches have been developed: either the amplitude of a static or dynamic point is modulated over time, or a static or dynamic

contour is repeatedly drawn on the user's skin by rapid motion of the focal point. The latter approach, which employs a technique known as spatio-temporal modulation (STM) [Frier et al. 2018; Kappus and Long 2018] or lateral modulation (LM) [Takahashi et al. 2018], has been the go-to for most work on 2D contour rendering with UMH [Georgiou et al. 2022; Matsubayashi et al. 2019; Mulot et al. 2023]. Yet, rendering 3D objects in full would mean that the interface's output energy is spread out over the whole shape, making it almost imperceptible. Current approaches thus mostly focus on rendering a representation of the intersection between the object and the user's hand [Long et al. 2014; Martinez et al. 2019] (see Fig. 1). But there is currently no consensus on what inherently constitutes a 3D object rendering algorithm, and how to make it. This makes it more challenging to discuss and compare these techniques.

Thus, in this paper:

- We formalize *intersection strategies*, describing the process of computing intersection representations based on hand and object information (Sec. 3). Combined with state-of-the-art techniques for rendering curves, this creates an end-to-end pipeline for designing 3D object rendering algorithms. We discuss implications for rendering performance (e.g. computation time and operating noise) and perception of virtual 3D objects (Sec. 4);
- We illustrate the importance of studying intersection strategies, researching whether differences between strategies influence the perception of virtual object properties. To that end, we discuss a state-of-the-art 3D rendering technique under the intersection strategy viewpoint. We also designed an example intersection strategy, following the intersection strategy pipeline (Sec. 4). *Based on user's feedback*, we evaluated through a *user study* the impact of the state-of-the art strategy and our new example strategy on users' perception of the infill density of virtual 3D objects (Secs. 5 and 6). The results demonstrate that well-designed intersection strategies can render challenging properties such as infill density.

Our work aims both to provide tools for standardising the algorithmic aspects of rendering 3D objects with UMH, and to experimentally demonstrate that intersection strategy design can have a significant impact on the perception of virtual object properties. By normalising reporting and studying methods, we hope to facilitate further exploration of perceptual effects related to 3D object rendering using UMH within the haptic community, but also the virtual reality and HCI communities.

2 RELATED WORK

UMH has applications in many manipulation tasks involving 3D virtual objects. For instance, Romanus et al. [2019] proposed a prototype system that enables mid-air tactile exploration of anatomical visualisations in mixed reality, Howard et al. [2019] proposed a UMH virtual reality (VR) demonstrator in which users can explore a variety of 3D objects, and Matsubayashi et al. [2019] proposed a system allowing physical manipulation of 3D objects in VR with UMH feedback.

For such tasks, it may initially appear easier to render the entire geometry of the 3D tactile objects simultaneously [Hasegawa and Shinoda 2013; Inoue et al. 2015; Korres and Eid 2016]. However, rendering 3D objects in full with UMH is almost never efficient, as users are rarely in contact with the whole object they are interacting with. Rather, only the surfacic parts of the object currently in contact with the skin need to be rendered. Furthermore, rendering 3D objects in full with UMH is quickly limited by issues of output pressure, achievable draw frequency, resolution, as well as the fact that the object's tactile contours appear poorly defined [Matsubayashi et al. 2019].

Therefore, the common solution for rendering 3D objects has been to render the local intersection of a user's hand with a given virtual object (see Fig. 2(A)). This technique generates a set of points and contours on the surface of the user's palm and fingers [Long et al. 2014; Martinez et al. 2019; Matsubayashi et al. 2019; Maunsbach et al. 2024; Mulot et al. 2024].

The method for transforming a theoretical geometric contour into an actual ultrasound tactile stimulus is well understood and referred to as the *sampling strategy*, a concept introduced by Frier et al. [2019] and later formalized by Mulot et al. [2021]. It is worth noting that any pattern-based UMH rendering algorithm technique (2D or 3D) uses some sort of *sampling strategy*, while 3D rendering algorithms require an additional preliminary step to compute the 2D pattern from the hand-object intersection. However, despite the existence of several prototype applications for rendering 3D objects by intersecting a user's hand with a virtual object [Howard et al. 2022; Long et al. 2014; Martinez et al. 2019; Matsubayashi et al. 2019; Maunsbach et al. 2024], there has not yet been a general formalization of the pipeline for going from said intersections to a 2D geometry that may be used as input for a chosen sampling strategy. These applications present a few ways to render 3D objects, but with no consensus on what inherently makes a 3D rendering scheme.

Our work aims to address this lack of consensus by formalizing *intersection strategies*. Combined with *sampling strategies*, this forms a two-part process to design a 3D object rendering technique with UMH. In doing so, we hope to facilitate the discussion of 3D mid-air rendering algorithms, by providing this baseline. We also highlight with a user study (Sec. 5, 6) that well-chosen intersection strategies render challenging 3D object properties (illustrated with infill density). We thus hope to motivate the mid-air haptic community to further explore and study these intersection strategies.

3 INTERSECTION STRATEGIES

An UMH rendering scheme for 3D objects requires two inputs at all times: the object to render and the configuration of the hand exploring it. Based on these inputs, we propose a generalized two-part process: an *intersection strategy* first interprets the hand-object intersection as a contour, then a *sampling strategy* [Frier et al. 2019; Mulot et al. 2021] uses the result to generate the spatiotemporal evolution of a focal point, defining an UMH stimulus. In this section, we formally define the representation of inputs and outputs (Sec. 3.1) and the generation and parameterization of an intersection strategy (Sec. 3.2).

3.1 Component Representations

The intersection strategy algorithm requires three components to be represented: the virtual object, the hand, and the resulting intersection.

The virtual object and hand are both virtual 3D objects, for which many representations, either implicit or explicit, exist [Lin and

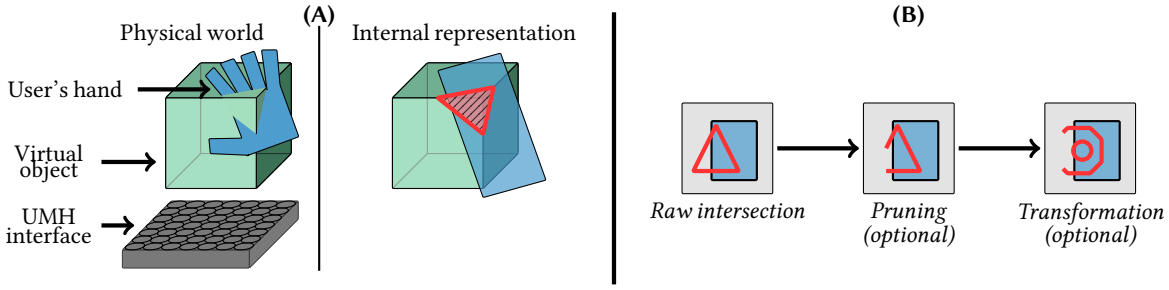

Figure 2: Overview of UMH rendering of a 3D Object. (A) Raw intersection (red) between a virtual object (green cube) and the hand's internal representation. (B) The three steps for applying an intersection strategy, given a virtual object and hand. First, we compute the outline of the intersection between the virtual object and the hand. Then, we optionally prune parts of the obtained contour, if they are not required. Finally, we optionally apply a transformation to the contour.

Gottschalk 1998]. Implicit representations often offer easy geometric collision computation, while explicit representations may be more convenient to generate and more intuitive to work with. But geometric collisions and intersections can be computed between any two representations, with state-of-the-art computer graphics algorithms [Lin and Gottschalk 1998], meaning that intersection strategies are agnostic regarding this aspect. If needed, classical object representations can also be augmented to contain additional information that could be useful to the rendering (e.g. local texture or physics-based representation).

It should be noted that regardless of the chosen data structure, it can often be computationally efficient to separate the visual representation (potentially high-resolution) from a collocated simplified representation used for intersection processing. For the object, these simplifications can be made on the basis of rendering resolution, e.g. there is no need to represent object details smaller than the size of a focal point [Rakkolainen et al. 2021]. This can serve as a guide to define an approximate implicit surface representation of an object, to choose voxel size or to set the level of mesh detail, for instance. For the hand, simplifications can be made based on the required areas of interaction. While some applications have used mesh representations of the hand [Long et al. 2014; Maunsbach et al. 2024], it is often more efficient and just as satisfactory to represent the hand through simple implicit surfaces, e.g. a plane [Mulot et al. 2023] or set of planes [Martinez et al. 2019; Mulot et al. 2024]. This is because UMH interaction mostly focuses on the glabrous skin of the palm and fingers, with interactions happening mostly with more open hands.

The representation choices will impact computational load, haptic rendering detail, as well as the resulting representation of the intersection. Regarding the latter, any resulting intersection representations need to be converted to a 3D curve to be usable as an input for the downstream sampling strategy [Mulot et al. 2021]. This is commonly done using sets of polylines, i.e., continuous sets of line segments connected at their extremities [Martinez et al. 2019]. These are particularly convenient when working with meshes, as they provide an exact representation of the intersection.

3.2 Definition of Intersection Strategies

We define the *intersection strategy* as the process of computing a contour which semantically represents the intersection between a hand and a 3D virtual object. This process follows three steps (see Fig. 2). The *raw intersection* computes the collision between the hand and virtual object, then the *pruning* removes unwanted parts of the feedback, and the *transformation* step modifies the obtained contours. These steps have been carefully chosen to facilitate the discussion of state-of-the-art 3D rendering techniques under the viewpoint of *intersection strategies*, while still allowing for the representation of any type of intersection technique.

Once the resulting contour has been computed using the intersection strategy, a *sampling strategy* [Mulot et al. 2021] can be applied to generate the sequence of focal points that will be rendered by the UMH interface. As sampling strategy's parameters can impact the user's haptic perception of a 2D stimulus [Frier et al. 2019; Mulot et al. 2021], we hypothesize that the parameters of the intersection strategy may also impact the user's perception of 3D objects, as well as other meta-parameters (e.g. computation time, noise produced).

3.2.1 Raw Intersection. In the case where hand and object are represented either both as implicit functions or both as voxels, evaluating the Boolean intersection is relatively straightforward. In other cases, either objects can be converted into convenient representations (e.g. voxelized), or a specific intersection algorithm must be selected based on the nature of the component representations. For example, considering palm and fingers as bounded planes in 3D space and virtual objects as meshes, a mesh-plane intersection algorithm (e.g. [Minetto et al. 2017]) can be used to produce a set of curves lying within the planes of the glabrous skin of the hand. If instead the hand and object representations generate a surfacic intersection, it is possible to turn it into one or several polylines, e.g. by following the algorithm from Maunsbach et al. [2024]

This raw intersection step (Fig. 2 (B-Left)) is mandatory, as it extracts the geometric features of the hand-object intersection. If the data structure for the object allows it, this step could also extract additional information (e.g. texture, feature) that could be used for the next intersection strategy steps, or downstream for the sampling strategy.

3.2.2 Pruning. The computed raw intersection may contain information that is not relevant when aiming for efficient rendering. An optional contour pruning step can therefore be useful to reduce the handled intersection contours down to the bare minimum required for efficient rendering and perception. For example, parts of the raw

intersection may end up lying at a distance from the skin (e.g. the circle in Fig. 3), where even if they were rendered, they would not be felt by the user. These parts could thus be removed. Also, as proposed by Martinez et al. [2019], and implemented by Mulot et al. [2024], we could remove segments that are too close to each other (e.g. when intersecting an object with small width), if users would not be able to distinguish them.

It should be noted that applying this step may transform continuous contours into discontinuous open patterns (see Fig. 2 (B-Center)) which in turn could lead to discontinuities in the focal point motion. This is a well-known source of operating noise for UMH interfaces [Georgiou et al. 2022].

3.2.3 Transformation. Finally, the raw or pruned contour may not be the most effective way of conveying the properties of an explored object. Haptic designers may want to transform the contour obtained after the previous two phases while conserving some of the obtained geometric information. The aim of this may be to use specific patterns (e.g. circles) whose perception is well-studied [Frier et al. 2019], to take advantage of interference effects [Reardon et al. 2023], or to highlight certain object features [Martinez et al. 2019]. Thus, a final optional transformation step completes the general definition of the intersection strategy (Fig. 2 (B-Right)).

3.2.4 Generalizability. We formalized the intersection strategy rendering pipeline in an effort to provide a baseline for future discussion about 3D object rendering with UMH. The underlying steps were also chosen to fit previous work in the field. This shows that the steps are well chosen, and ensures easy comparisons of rendering techniques. For instance, the 3D aspect in the work of Long et al. [2014], and Matsubayashi et al. [2019] was mostly centered on the raw intersection, while the proposed techniques by Martinez et al. [2019] could be interpreted as a basic raw intersection, combined with different transformation steps.

Furthermore, given that collisions can be computed between any two object representations, and since the last step can represent any arbitrary transformation, the generalizability of this rendering pipeline is ensured.

Overall, in this section we formalised *intersection strategies*, the first part prior to the *sampling strategy* when rendering a 3D object with UMH. *Intersection strategies* are the succession of a *raw intersection*, *pruning*, and *transformation* step, ensuring its generalizability. In doing so, we enable easier discussions and exploration of 3D object rendering with UMH, and deeper exploration of their perceptual applications.

4 USING INTERSECTION STRATEGIES TO GENERATE HAPTIC RENDERING SCHEMES

To *illustrate the intersection strategy process*, we designed example haptic rendering schemes using the previously described formalization, to explore whether differences between strategies affect the perception of virtual object properties (Sec. 5, 6). We followed an *exploratory approach*, designing these example strategies and asking participants how they would interpret the haptic feedback difference, in order to find the direction of the following user study.

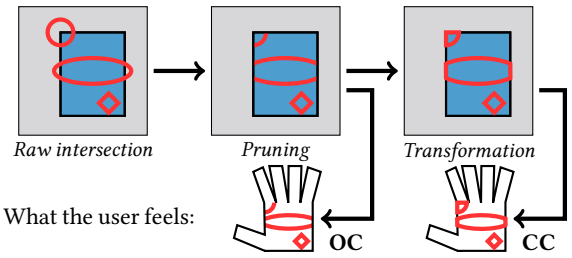

Figure 3: We designed an intersection strategy, following the process of Fig. 2. After the plane-mesh intersection has been computed (red), parts that are outside of the hand rectangle (blue), are removed during the pruning step. Then, segments are added along the rectangle contour to close the open contours. We call OC and CC the feedback obtained after the pruning and transformation steps, respectively (Sec. 3.2).

4.1 Intersection Strategies

We first consider a basic intersection strategy, which uses only the default raw intersection step and a pruning step that removes contours that are outside the boundaries of the hand. With this strategy, partial intersections of an object by the hand causes the user to feel sets of open contours (see Fig. 3) which users are free to interpret in any way they wish. This is equivalent to some state-of-the-art rendering techniques for 3D object rendering (e.g. strategy A by Martinez et al. [2019]), and serves here as a comparison baseline.

We then design a derived intersection strategy where we perform an additional transformation step to systematically close intersection contours so that they encapsulate the "inside" of the intersected virtual object (see Fig. 3). In the remainder of this paper, we refer to the first intersection strategy as **OC** (**O**pen **C**ontour) and the second intersection strategy as **CC** (**C**losed **C**ontour).

While **OC** is a state-of-the-art baseline, presented here under the intersection strategy pipeline, **CC** is a novel haptic rendering scheme, the purpose of which is to illustrate how different intersection contours may affect a user's interpretation of virtual object properties (e.g. geometry or fill density).

4.2 Chosen Component Representations

For these haptic rendering schemes, we represented virtual objects as meshes. We chose to instruct users to explore objects with their palm only. This approach simplified the hand to a single rectangle covering the palm, which could easily be implicitly represented. This decision was made to reduce the computational cost and ensure a consistent feedback between participant, regardless of the shape of their hand. However, it is important to note that the concepts presented in this paper still apply to other representations, although more work is required to understand how they impact the user's perception.

Once the final pattern is obtained, we apply a sampling strategy that uses STM with a focal point speed of 7 m/s [Frier et al. 2018, 2019].

4.3 Effects on Non-Haptic Factors

By closing the contour, we render some additional segments that are inside the virtual object, which could have several implications beyond a user's perception of the object. For instance, given the

constant-speed sampling strategy we used, rendering these longer patterns means that the **CC** feedback will be rendered at a lower draw frequency than the equivalent **OC** feedback.

4.3.1 Computation Time. In general, the use of different algorithms or parameters for the different steps of the intersection strategy may impact the computation time. For **CC** and **OC**, with a naive C# implementation running on a 12th Gen Intel Core i7-12700H CPU, we measured that the raw intersection step takes about 1 ms per 100 mesh faces, while the pruning step requires about 0.2 ms per 100 mesh faces, and the transformation step for **CC** requires less than 0.1 ms in total. That said, performances could be greatly improved by using a GPU, but we do not expect that a significant difference would appear between the **CC** and **OC** computation time.

4.3.2 Operating Noise. When an open contour is drawn using STM, the spatial discontinuities of the focal point path generate high-pitch audible harmonics, which may not be pleasant. By closing the contour, the number of spatial discontinuities is reduced, thus reducing the generated noise. To assess this, we positioned a Shure SM58 microphone 7 cm above and 15 cm to the side of the haptic interface, connected to a Focusrite Scarlett 2i2 sound card, with 96 kHz sample rate. A 13 cm-wide virtual cube was centered 20 cm above the interface. We recorded the noise produced by a 30 s exploration of this cube with both the **CC** and **OC** feedback. This recording was performed ten times. After that, we measured the differences in peak and RMS sound pressure levels for the **OC** and **CC** recordings. This resulted in **OC** being on average 0.54 dB (RMS) louder than **CC**, while having peaks 1.9 dB lower. That said, these differences were not significantly different from 0 (Shapiro, $p > 0.05$, one-sample t-test, $p > 0.05$).

We also computed the Fourier spectrum for each recording, as illustrated in Fig. 4. From these, we observe that the discontinuities in the **OC** feedback lead to the generation of higher frequency harmonics in the 300 Hz - 10 kHz band, explaining the higher perceived pitch for the noise generated by **OC**. This is also coherent with the slightly higher RMS level for **OC**. Since humans perceive frequencies between 300 Hz and 10 kHz as louder than lower frequencies [Suzuki and Takeshima 2004], the **OC** feedback appears louder and less pleasant [Patchett 1979].

5 PILOT STUDY: IMPACT OF HAPTIC RENDERING SCHEMES ON PERCEIVED SHAPE PROPERTIES

To highlight the importance of studying intersection strategies, we used the previously described **OC** and **CC** rendering schemes in a pilot study to initiate the exploration of the perception and interpretation of these stimuli. It is worth noting that **OC** and **CC** were designed to *illustrate the intersection strategy pipeline* rather than to render specific properties. So this pilot aims to understand whether participants feel a difference between the two rendering schemes, and how they would interpret this difference in terms of object properties. This will then allow us to study the impact of the two feedbacks on these relevant properties (Sec. 6).

5.1 Materials and Methods

5.1.1 Apparatus and Setup. Participants were seated facing the laptop running the experiment software, and an Ultraleap Stratos Explore[1] haptic interface was placed next to the laptop on the side of the participants' dominant hand, (Fig. 5(A)). The participant's dominant hand, with which they explored the virtual objects in the experiment, was tracked using an Ultraleap StereoIR 170 camera[2]. The experiment software was designed and run using Unity[3] 2022.3.9f1.

5.1.2 Procedure and Collected Data. This preliminary study comprised 5 trials, for five virtual shapes: a tube, a sphere, a dog, a cube, and a rock, in this order (see Fig. 5(B)). The shapes were all designed to fit inside a 13 cm wide cube whose centroid was positioned 20 cm above the UMH interface. This ensured that the entirety of the shape was inside the workspace of both the hand tracker and the haptic interface. For each trial, the participant performed two successive 20 s free explorations of the virtual object displayed on the laptop's screen, rendered once with **OC** and once with **CC**.

After these two explorations, they answered the following three open questions:

1) Did the haptic stimuli feel different? If so, how?
2) Did the virtual objects feel physically different? If so, how?
3) Was there a difference in terms of perceived coherence between the tactile sensation and the object's visual aspect?

5.1.3 Participants. Six participants (6 M, age: 24.2 ± 2.2 y.o.) took part in this pilot experiment. Four were right-handed and two were left-handed. One was very experienced with haptics, four reported limited experience with haptics, and one had almost no experience. Five of them had already felt an ultrasound haptic stimulus in the past.

5.2 Results and Discussion

We observed that two participants were always able to perceive a difference between the two rendering schemes, while two participants failed to perceive a difference once, and two participants failed to perceive a difference twice (out of 5 trials). This seems to reveal a relatively clearly apparent perceptual difference between the two rendering schemes. Deeper investigation in a larger and more diverse population would be necessary to evaluate how the different parameters influence the perception of these stimuli. For instance, some participants reported "differences in terms of geometry" as the **CC** scheme renders segments that are not part of the original shape's contour, while other participants mentioned differences in terms of perceived "frequency", as the difference in length between the patterns computed by the two schemes led to different haptic draw frequencies. Some participants also interpreted this change in draw frequency as a textural difference between the two patterns, with **OC** feeling "smoother" than **CC**. This is coherent with the results of Wojna et al. [2023] and Ablart et al. [2019], who showed that texture roughness and draw frequency are negatively correlated.

We also observed differences between shapes. Most participants perceived the biggest differences while intersecting with the cube or the sphere. Since both these shapes have convex geometries with

[1] https://www.ultraleap.com/datasheets/STRATOS_Explore_Development_Kit_datasheet.pdf
[2] https://www.ultraleap.com/product/stereo-ir-170/
[3] https://unity.com/fr

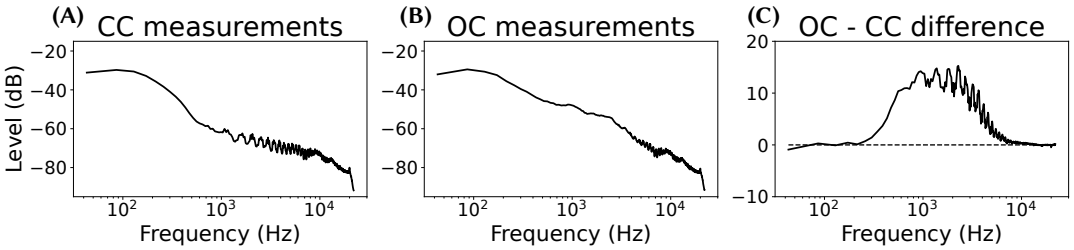

Figure 4: (A) (resp. (B)) Fourier transforms of the audio recordings during an interaction with CC (resp. OC) feedback. (C) Difference between the (A) and (B) spectra: OC generates more energy than CC in the 300 - 10 kHz band and less energy below 300 Hz. All spectra are the result of averaging ten measurements.

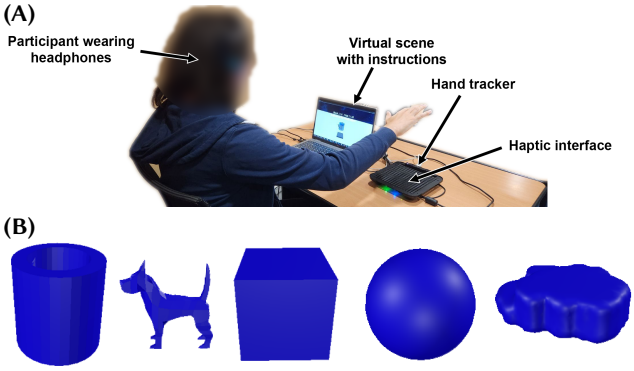

Figure 5: (A) Experimental setup for the pilot study (Sec. 5) and user study (Sec. 6): participants seat facing the screen, interacting with their dominant hand above the UMH interface. They wear headphones to mask exterior noises. (B) Participants explored different 3D objects, namely a tube, a dog, a cube, a sphere, and a rock. The first three were used in both the pilot (Sec. 5) and user study (Sec. 6), while the last two were only used in the pilot.

larger inner volumes, the differences in length between both intersection patterns may be more pronounced. This leads to a larger difference in stimulated skin area and in draw frequency. The combination of these factors could explain this observed effect.

When interpreting the haptic differences in terms of physical properties of the virtual objects, the participants mentioned a variety of parameters. Two participants mentioned "geometric differences," while one participant reported that **OC** gave a sensation of a contour rendering, interpreting the shape as hollow, while **CC** rendered surfaces, leading to the sensation of something filled. They also mentioned an impact on the "solidity," "density," and "smoothness" of the object. Overall, the most cited parameter was the density and filling of the object, which was mentioned at least once by every participant. This is coherent with the larger stimulated area from **CC**, which can be interpreted as the presence of more physical matter. In the rest of this presentation, we refer to this property as infill density.

The majority of answers from five of the six participants indicated that the **CC** rendering scheme was perceived as more coherent with the virtual objects' visual aspect.

Given the motivations for this study and low amount of participants, these results are to be interpreted as a way to guide our next study, presented in Sec. 6, with hints towards potential perceptual effects that would need further investigation.

6 USER STUDY: MODIFYING THE PERCEPTION OF INFILL DENSITY

In light of the results of the pilot experiment (Sec. 5), we designed a user study to further study the impact of the rendering scheme on the perception of an object's infill density, as it was the most referenced property in the pilot study. We hypothesize that shapes rendered with **CC** will be felt as more densely filled than shapes rendered with **OC**.

6.1 Materials and Methods

6.1.1 Apparatus and Setup. We used a similar setup to that of the pilot experiment (Sec. 5, Fig. 5(A)), with participants seated facing the experiment laptop and haptic interface. They wore a headset playing pink noise to mask the UMH interface operating noise.

We used three virtual objects: a cube, a tube, and a dog. The cube and tube used the same mesh for the visual and haptic representations, with 12 and 256 triangles respectively, while the dog used a relatively detailed (1160 triangles) visual representation, and a simplified (136 triangles) collocated haptic representation.

6.1.2 Procedure. The experiment was divided into six blocks, one for the exploration of each object with one of two visual representations (opaque or semi-transparent with an opacity of 70%). We used this transparency factor as it may be a way to visually suggest the infill density of the object, and its effect may interact with that of the haptic feedback.

Blocks followed a 2-IFC protocol: participants explored the object for 7 s with either the **CC** or **OC** haptic rendering before exploring it a second time with the other one. After that, they answered the following question: "Which one of the two shapes felt the most densely filled?" using the keyboard's left and right arrow keys. The answer corresponding to each key ("First"/"Second") randomly changed between trials and was also written on the screen for the participants to see. Five repetitions of each rendering order were presented in a random sequence, yielding 10 trials per block. The block order was randomized using a Latin square.

6.1.3 Collected Data. For each trial, we collected the participant's answer. After each block, participants also rated their confidence in

their answers and the perceived difficulty of the task on a 7-point Likert scale.

During each of the explorations with **CC**, we also measured the ratio r between the average length of the patterns computed using the **CC** intersections strategy, and those that would be computed using **OC** during the same exploration. Given that **CC** adds contours compared to **OC**, r is always greater than 1. This measure relates to how physically different the two schemes are.

6.1.4 Participants. We recruited 18 participants (15 M, 2 F, 1 NB, age: 26.9 ± 5.8 y.o.), who had not participated in the pilot study. One was left-handed, and all others were right-handed. Four participants were experienced with haptics, while eight participants reported having limited experience, and six had little to no prior experience. Ten participants had never used an UMH device before.

6.2 Results

For each participant and each block, we computed the proportion p_{CC} of answers indicating that the **CC** feedback gave the impression of a more densely filled object. The results for each shape and visual levels are illustrated in Fig. 6.

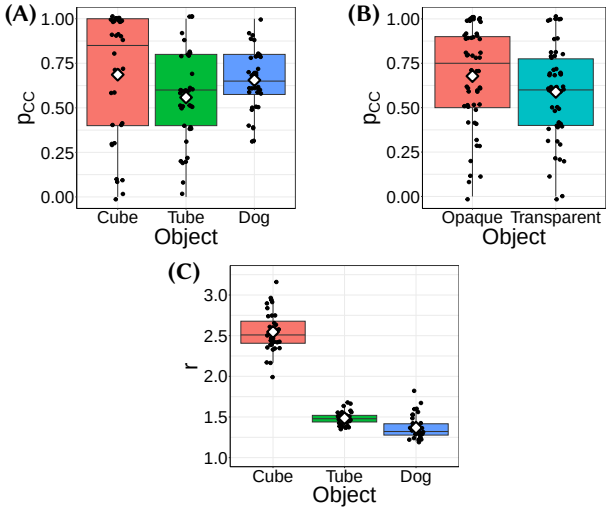

Figure 6: (A) Distribution of the proportion of answers p_{CC}, reporting that the object rendered with CC felt more densely filled than the one rendered with OC. (B) Distribution of p_{CC} per visual representation. (C) Distribution of the ratios r between the average CC pattern length and their OC equivalent. Black dots represent measurements per participant per block, and white diamonds represent the means.

As the p_{CC} data did not follow a normal distribution (Shapiro, $p < 0.001$), we performed a one-sample Wilcoxon signed rank test, showing that p_{CC} is significantly higher than the 50% chance-level ($p < 0.001$). Pairwise Wilcoxon tests with Holm corrections revealed that the cube had significantly higher p_{CC} scores ($p = 0.03$) than the tube. A Wilcoxon test also revealed that p_{CC} was significantly higher for opaque shapes than for transparent ones ($p = 0.006$).

Holm-corrected pairwise Wilcoxon tests showed that the r distributions were significantly different for all three objects ($p < 0.001$ for all comparisons).

Looking at the individual participant data, 12 participants had at least 5 out of 6 p_{CC} results at 0.5 or higher, showing a strong tendency to report the **CC** feedback as giving the impression of a more densely filled object. 3 participants had opposite results, and 3 participants had ambiguous results revolving around the 0.5 chance level.

Holm-corrected pairwise Wilcoxon tests showed that participants were more confident in their answers for the cube than for the dog or the tube (respectively $p = 0.005$, $p = 0.012$). Similarly, they also found the task easier with the cube ($p = 0.004$ for both comparisons). On the contrary, the opacity had no significant impact on the confidence and perceived difficulty (Wilcoxon, $p = 0.05$ for both comparisons).

6.3 Discussion

In this study, we hypothesized that shapes rendered with **CC** will be perceived as more densely filled than shapes rendered using **OC**. Since p_{CC} is significantly higher than the chance level, this hypothesis is fully supported. This is also coherent with the results from the pilot study.

The p_{CC} distribution for the cube shows a high variance. However, it is important to note that the p_{CC} data appear to form a bimodal distribution, hinting at the presence of two subgroups within the population who interpret the relationship between intersection contour and shape infill density in opposite manners. The significantly high r for this shape indicates a particularly strong difference between **OC** and **CC** feedback, which was thus easy to perceive. Therefore, depending on the participant's interpretation of the feedback, their p_{CC} value tends to be closer to 0 or 1, but further away from the 0.5 chance level, thus increasing the variance. This is also coherent with the higher p_{CC}, and confidence level observed for the cube. To better understand this effect, it would be interesting to conduct a similar experiment with other sampling strategies (e.g. constant draw frequency) to study whether the perceived difference is mostly due to the difference in terms of actual drawn contour, or to the difference in resulting draw frequency.

On a similar topic, it is important to note that by altering the properties of the rendered pattern (e.g. size, geometry), we also alter the range of different sampling parameters (e.g. we can likely use slower focal point patterns on shorter path. Future work will be dedicated to study how intersection strategies and sampling strategies influence each other.

The per-participant results also seem to hint towards the presence of two distinct subgroups, depending on their interpretation of the haptic difference between **OC** and **CC**. Most participants appear to easily discriminate **CC** and **OC**, but their interpretations vary. This was partly confirmed by free comments given by participants after completing the experiment. Also, similarly to what was observed in the pilot, some participants reported feeling differences in other properties than infill density (e.g., roughness or stimulus area).

A larger and more diverse sample would be required to confirm the existence of subgroups and to assess their proportions within the population. While this experiment showed that haptically rendering virtual objects with different intersection strategies can create differences in perceived object properties, future work could investigate

the factors determining participants' interpretations of intersection strategies.

Very interestingly, the opaque visual led to higher p_{CC} values, but did not significantly impact the user's confidence or perceived difficulty, which seems to indicate that the effect may be unconscious. This could also emerge from a visuo-haptic effect, where the opaque object may be expected to be more densely filled, confirming the participant's haptic perception. That said, deeper investigations with more participants would be required to test those hypotheses.

Given the low intensity provided by UMH devices, rendering solid objects has always been a struggle. This experiment showed that by altering the intersection strategy, we can improve the perception of such properties. Furthermore, the pilot study also seemed to indicate that this feedback is also felt as more coherent with the visual of the object, despite the rendering of segments that are not part of the initial shape's outline. That said, deeper experiments should be conducted to confirm this last result.

7 CONCLUSIONS AND PERSPECTIVES

The 3D workspace of ultrasound mid-air haptic (UMH) devices makes them particularly suited to rendering 3D virtual objects. In an effort to formalize the process of 3D object rendering with UMH, we propose the concept of intersection strategies: a high-level algorithmic approach to compute sets of curves representing a hand-object intersection. Paired with the existing formalism of sampling strategies for rendering curves, this provides an end-to-end process for generating UMH stimuli based on the exploration of 3D virtual objects. We hope this formalism can assist future UMH interaction designers, as well as provide a basis for studying and discussing the perceptual impacts of intersection strategy design choices.

To emphasize the importance of studying the different steps of intersection strategies, we designed a new haptic rendering scheme, and followed an exploratory methodology to compare it to a state-of-the-art scheme. We showed that acting on the transformation step can affect users' perception of virtual object's infill density. Furthermore, we assessed the impacts of these rendering schemes on UMH interface operating noise.

We observed that a majority of users interpreted the abstract feedback in the same way, however more detailed user studies would be required to study whether subgroups exist in the population as well as to understand the parameters affecting their interpretations of virtual object properties. Also, future studies could study the potential impacts of other more complex intersection strategy designs on the perception of other virtual object properties, and look into the rendering of other volumetric properties. We will also investigate the dependencies between intersection strategies and sampling strategies.

ACKNOWLEDGMENTS

This work was funded by the European Union (ERC, ADVHANDTURE, 101088708).

REFERENCES

William Ablart, Damien Frier, Hannah Limerick, Orestis Georgiou, and Marianna Obrist. 2019. Using ultrasonic mid-air haptic patterns in multi-modal user experiences. In *Proc. IEEE HAVE*. 1–6.

Sue Ann Carter, Tom Seah, Benjamin Long, Bruce Drinkwater, and Sriram Subramanian. 2013. UltraHaptics: multi-point mid-air haptic feedback for touch surfaces. In *Proc. ACM Symp. UIST*. 505–514.

William Frier, Damien Ablart, Jamie Chilles, Benjamin Long, Marcello Giordano, Marianna Obrist, and Sriram Subramanian. 2018. Using spatiotemporal modulation to draw tactile patterns in mid-air. In *Proc. Eurohaptics Conf.* 270–281.

William Frier, Dario Pittera, Damien Ablart, Marianna Obrist, and Sriram Subramanian. 2019. Sampling strategy for ultrasonic mid-air haptics. In *Proc. ACM CHI Conf.* 1–11.

Orestis Georgiou, William Frier, Euan Freeman, Claudio Pacchierotti, and Takayuki Hoshi. 2022. *Ultrasound Mid-Air Haptics for Touchless Interfaces.* Springer.

Keisuke Hasegawa and Hiroyuki Shinoda. 2013. A method for distribution control of aerial ultrasound radiation pressure for remote vibrotactile display. In *Proc. SICE*. 223–228.

Takayuki Hoshi, Takayuki Iwamoto, and Hiroyuki Shinoda. 2009. Non-contact tactile sensation synthesized by ultrasound transducers. (2009), 256–260.

Thomas Howard, Maud Marchal, Anatole Lécuyer, and Claudio Pacchierotti. 2019. PUMAH: pan-tilt ultrasound mid-air haptics for larger interaction workspace in virtual reality. *IEEE Trans. Haptics* 13, 1 (2019), 38–44.

Thomas Howard, Maud Marchal, and Claudio Pacchierotti. 2022. Ultrasound mid-air tactile feedback for immersive virtual reality interaction. In *Ultrasound Mid-Air Haptics for Touchless Interfaces*, Orestis Georgiou et al. (Eds.). 147–183.

Seki Inoue, Yasutoshi Makino, and Hiroyuki Shinoda. 2015. Active touch perception produced by airborne ultrasonic haptic hologram. In *Proc. IEEE WHC*. 362–367.

Takayuki Iwamoto, Mari Tatezono, and Hiroyuki Shinoda. 2008. Non-contact method for producing tactile sensation using airborne ultrasound. (2008), 504–513.

Brian Kappus and Ben Long. 2018. Spatiotemporal modulation for mid-air haptic feedback from an ultrasonic phased array. *The Journal of the Acoustical Society of America* 143, 3 (2018), 1836–1836.

Georgios Korres and Mohamad Eid. 2016. Haptogram: Ultrasonic point-cloud tactile stimulation. *IEEE Access* 4 (2016), 7758–7769.

Ming Lin and Stefan Gottschalk. 1998. Collision detection between geometric models: A survey. In *Proc. IMA conference on mathematics of surfaces*, Vol. 1. 602–608.

Benjamin Long, Sue Ann Seah, Tom Carter, and Sriram Subramanian. 2014. Rendering volumetric haptic shapes in mid-air using ultrasound. *ACM Trans. Graphics* 33, 6 (2014), 1–10.

Adam Martinez, Jonatan Harwood, Hannah Limerick, Rory Clark, and Orestis Georgiou. 2019. Mid-air haptic algorithms for rendering 3d shapes. In *Proc. IEEE HAVE*. 1–6.

Atsushi Matsubayashi, Yasutoshi Makino, and Hiroyuki Shinoda. 2019. Direct finger manipulation of 3D object image with ultrasound haptic feedback. In *Proc. ACM CHI Conf.* 1–11.

Martin Maunsbach, William Frier, and Kasper Hornbæk. 2024. MAMMOTH: Mid-Air Mesh-based Modulation Optimization Toolkit for Haptics. In *Proc. ACM CHI Conf.* 1–7.

Rodrigo Minetto, Neri Volpato, Jorge Stolfi, Rodrigo MMH Gregori, and Murilo VG Da Silva. 2017. An optimal algorithm for 3D triangle mesh slicing. *Computer-Aided Design* 92 (2017), 1–10.

Lendy Mulot, Guillaume Gicquel, Quentin Zanini, William Frier, Maud Marchal, Claudio Pacchierotti, and Thomas Howard. 2021. Dolphin: A framework for the design and perceptual evaluation of ultrasound mid-air haptic stimuli. In *Proc. ACM SAP*. 1–10.

Lendy Mulot, Thomas Howard, Guillaume Gicquel, Claudio Pacchierotti, and Maud Marchal. 2024. Bimanual Ultrasound Mid-Air Haptics for Virtual Reality Manipulation. *IEEE Transactions on Visualization and Computer Graphics* (2024), 1–11.

Lendy Mulot, Thomas Howard, Claudio Pacchierotti, and Maud Marchal. 2023. Improving the Perception of Mid-Air Tactile Shapes With Spatio-Temporally-Modulated Tactile Pointers. *ACM Trans. Applied Perception* 20, 4 (2023), 1–16.

Robin F Patchett. 1979. Human sound frequency preferences. *Perceptual and motor skills* 49, 1 (1979), 324–326.

Ismo Rakkolainen, Euan Freeman, Antti Sand, Roope Raisamo, and Stephen Brewster. 2021. A survey of mid-air ultrasound haptics and its applications. *IEEE Trans. Haptics* 14, 1 (2021), 2–19.

Gregory Reardon, Bharat Dandu, Yitian Shao, and Yon Visell. 2023. Shear shock waves mediate haptic holography via focused ultrasound. *Science Advances* 9, 9 (2023), 1–9.

Ted Romanus, Sam Frish, Mykola Maksymenko, William Frier, Loïc Corenthy, and Orestis Georgiou. 2019. Mid-air haptic bio-holograms in mixed reality. In *Proc. IEEE ISMAR*. 348–352.

Yoiti Suzuki and Hisashi Takeshima. 2004. Equal-loudness-level contours for pure tones. *The Journal of the Acoustical Society of America* 116, 2 (2004), 918–933.

Ryoko Takahashi, Keisuke Hasegawa, and Hiroyuki Shinoda. 2018. Lateral modulation of midair ultrasound focus for intensified vibrotactile stimuli. In *Proc. EuroHaptics Conf.* 276–288.

Ronald T Verrillo. 1966. Vibrotactile sensitivity and the frequency response of the Pacinian corpuscle. *Psychonomic Science* 4, 1 (1966), 135–136.

Katarzyna Wojna, Orestis Georgiou, David Beattie, Michael Wright, and Christof Lutteroth. 2023. Does it par-tickle?: Investigating the relationship between mid-air haptics and visual representations of surface textures. *IEEE Trans. Haptics* 16, 4 (2023), 561–566.